Available online at www.sciencedirect.com
ScienceDirect
Journal of Microbiological Methods 67 (2006) 534 – 542
Journal of Microbiological Methods
www.elsevier.com/locate/jmicmeth

Real-time PCR assay to quantify *Fusarium graminearum* wild-type and recombinant mutant DNA in plant material

Rex B. Dyer *, David F. Kendra, Daren W. Brown

USDA Agricultural Research Service, National Center for Agricultural Utilization Research, United States

Received 28 February 2006; received in revised form 16 May 2006; accepted 16 May 2006
Available online 20 July 2006

Abstract

Fusarium graminearum (teleomorph, *Gibberella zeae*) is the predominant causal agent of Fusarium head blight (FHB) of wheat resulting in yearly losses through reduction in grain yield and quality and accumulation of fungal generated toxins in grain. Numerous fungal genes potentially involved in virulence have been identified and studies with deletion mutants to ascertain their role are in progress. Although wheat field trials with wild-type and mutant strains are critical to understand the role these genes may play in the disease process, the interpretation of field trial data is complicated by FHB generated by indigenous species of *F. graminearum*. This report describes the development of a SYBR green-based real time PCR assay that quantifies the total *F. graminearum* genomic DNA in a plant sample as well as the total *F. graminearum* genomic DNA contributed from a strain containing a common fungal selectable marker used to create deletion mutants. We found our method more sensitive, reproducible and accurate than other similar recently described assays and comparable to the more expensive probe-based assays. This assay will allow investigators to correlate the amount of disease observed in wheat field trials to the *F. graminearum* mutant strains being examined.
Published by Elsevier B.V.

Keywords: *Fusarium graminearum*; Fusarium head blight; Plant pathogen; Quantitative assay; Real-time PCR; SYBR green; Wheat scab

1. Introduction

Fusarium head blight (FHB), or scab, is a disease of cereal grains caused primarily by the fungal pathogen *Fusarium graminearum* (Bai and Shaner, 1994). Epidemics are intermittent in growing areas that have a humid to semi-humid climate and can significantly impact the wheat and barley industry (Bai and Shaner, 1994; Snijders, 1990). Economic losses result from a reduction in yield, poor seedling germination and contamination of seed with fungal toxins such as deoxynivalenol (DON), nivalenol (NIV) and zearalenone. Contaminated seed may be refused by livestock, cause a variety of animal diseases and necessitate expensive screening programs during grain preparation to exclude the toxins (Bai and Shaner, 1994; Snijders, 1990; Tuite et al., 1990).

Numerous virulence factors have been identified and characterized to varying degrees for *F. graminearum* (Dyer et al., 2005; Hou et al., 2002; Jenczmionka et al., 2003; Jenczmionka and Schafer, 2004; Lu et al., 2003; Seong et al., 2005; Urban et al., 2003; Voigt et al.,

* Corresponding author.
E-mail address: dyerr@ncaur.usda.gov (R.B. Dyer).

0167-7012/$ - see front matter. Published by Elsevier B.V.
doi:10.1016/j.mimet.2006.05.011

2005). The best studied virulence factor is the mycotoxin DON (Desjardins et al., 2000; Proctor et al., 1995; Rocha et al., 2005). DON toxicity to plants and animals is mediated through the inhibition of protein synthesis by interfering with ribosomal peptidyl transferases (Miller and Ewen, 1997). Wheat disease assays with DON mutants in the greenhouse and in the field have shown the important role DON plays in the disease process. Unfortunately, interpretation of the field trial data was complicated by a significant incidence of disease in control plots, generated presumably by indigenous strains of *Fusarium* including *F. graminearum* (Desjardins et al., 1996; Bai et al., 2001). Disease assessments, either FHB or toxin levels, do not provide any knowledge, *a prior*, of the fungi responsible.

Rapid advances in fungal genomic resources and technologies have led, at an unprecedented rate, to the identification of potentially new candidate virulence genes. Targeted gene disruption of the candidate genes is an important first step to assess function. The *Escherichia coli* hygromycin-B phosphotransferase gene (*HYG*), which confers resistance to the fungicide hygromycin, is a selectable marker frequently used with fungi and has been used to create a DON deficient strain of *F. graminearum* (Fincham, 1989; Proctor et al., 1995).

We describe the development of an easy and rapid, SYBR green-based real-time PCR assay for the quantification of total *F. graminearum* DNA and quantification of total *F. graminearum* DNA contributed by *HYG* tagged strains contained in DNA extracted from plant material. We found that our protocol is at least an order of magnitude more sensitive than previous SYBR green-based real-time quantitative PCR assays and is comparable in sensitivity to more expensive and complicated Taqman assays.

2. Methods

2.1. Fungal strains and culture conditions

F. graminearum strain FGSC 8630 (GZ3639) was isolated from scabby wheat in Kansas and is the progenitor strain for the two mutant strains, ΔFgOrfA-C15 (dAC) and ΔMat14 (dMat), examined in this work (Bowden and Leslie, 1992; Brown et al., 2004; Desjardins et al., 2004). All three strains produce DON in culture and *in planta*. dAC lacks a 4.5 kb portion of genomic DNA that includes the three open reading frames (ORFs) downstream of *TRI8*. dMat lacks a 9.6 kb portion of genomic DNA that includes the 4-gene MAT locus required for sexual reproduction. Hygromycin-resistant transformants were maintained on V-8 juice agar slants containing 300 μg ml^{-1} hygromycin B (Sigma, St. Louis, MO) and GZ3639 was maintained on V-8 juice agar slants.

2.2. Growth of wheat

Wheat (*Triticum aestivum* L.) cultivar Wheaton was grown in 18.7 cm plastic pots containing large coffee filters and filled with pasteurized soil (Scotts Redi-Earth Plug and Seedling Mix, Scotts Company, Marysville, OH). The pots were placed into the growth chamber (EconoAir, Model GC-16, Ecological Chambers, Inc., Winnipeg, Mb, Canada) and incubated at 15 °C with a 12 h light/dark cycle. Seedlings were fertilized with 200 ml pot^{-1} of an aqueous solution containing 1.25 g L^{-1} Peter's 20–20–20 (Spectrum Brands, St. Louis, MO) and 0.08 g L^{-1} Iron (II) Sulfate (Sigma, St. Louis, MO). After 4 to 5 weeks, pots were transferred to the greenhouse where temperatures were maintained at 23 °C during the day and 17 °C during the night. After a week, seedlings were thinned to four plants per pot. Plants were watered daily and fertilized weekly.

2.3. Production of fungal infected wheat seed

Fungal inoculum was prepared as described (Bai and Shaner, 1996). Briefly, macroconidia were generated by growth in 50 ml of mungbean media with shaking (200 rpm) at 25 °C for 4 to 5 days. Mungbean media was prepared by boiling 40 g of mungbeans in 1 L of deionized water for 10 min., filtering the resulting liquid through Miracloth (Calbiochem, EMD Biosciences, Inc., San Diego, CA) and autoclaving the filtrate. Macroconidia were harvested by low speed centrifugation and rinsed once with water. Spore concentrations were determined by hemacytometer and adjusted to 100,000 spores ml^{-1}. The third or fourth floret up from the base of the wheat head was inoculated by injection with either sterile water or with 1000–2000 macroconidia (10–20 μl from the 100,000 spores ml^{-1} stocks). After inoculation, wheat heads were enclosed in plastic bags (3 to 4 heads per bag) for three days to increase the humidity and encourage disease. Disease assessments were noted at 3 day intervals out to 21 days. Heads were allowed to mature prior to harvest and were individually threshed. Seeds from each treatment protocol (10 heads) were pooled, chopped into small pieces in a model M-2 Stein Laboratory Mill (Steinlite Corporation, Atchison, KS) and ground to a fine powder with a mortar and pestle.

2.4. DNA isolation

Fungal mycelia for DNA extraction was grown in GYP medium (20 g L^{-1} Glucose, 10 g L^{-1} Peptone, 3 g L^{-1} Yeast Extract) for 5 days at 25 °C with shaking (200 rpm). Mycelia was collected on Whatman 150 mm paper (Whatman International Ltd., Kent, UK) by filtration, rinsed with water and lyophilized. DNA was extracted using the DNeasy Plant Maxi Kit (Qiagen, Inc., Valencia, CA) according to the manufacturers' instructions. DNA concentration was determined by absorbance at 260 nm (OD_{260}). Absorbance readings were converted to concentration values (mass volume^{-1}) from a standard curve. The standard curve was produced by plotting the OD_{260} of serially diluted commercial DNA (1 kb Plus DNA Ladder, Invitrogen, Carlsbad, CA) vs. DNA concentration. DNA from wheat was extracted from 0.2 g of processed seed using the protocol and reagents in the Plant Maxi Kit from Qiagen. Purified DNA was quantified by relating the absorbance at 260 nm to the standard curve.

2.5. Primers

The *F. graminearum* species specific primers, Fg16 forward (Fg16F; 5'-CTCCGGATATGTTGCGTCAA-3') and reverse (Fg16R; 5'-GGTAGGTATCCGA-CATGGCAA-3'), amplify a 410 bp product (Nicholson et al., 1998). The *E. coli* hygromycin-B phosphotransferase specific primers (HygF5; 5'-AAGACCTGCCT-GAAACCGAAC-3' and HygR5; 5'-AAGAAGA-TGTTGGCGACCTCG-3') amplify a 400 bp product. The Fg16 primers were synthesized by Invitrogen (Carlsbad, CA) and purified by HPLC. The Hyg primers were synthesized by Sigma-Genosys (Woodlands, TX) and purified by HPLC. Lyophilized primers were dissolved in water to a concentration of 30 μM (Fg16 primers) or 60 μM (Hyg primers) and were stored at −20 °C.

2.6. PCR reaction conditions and cycling parameters

PCR reactions were set up in 0.2 ml white opaque low-profile polypropylene tubes and covered with ultra clear caps (Biorad Laboratories, Inc., Hercules, CA) in a final volume of 20 μl. Each sample contained 10 μl of 2× DyNAmo SYBR Green qPCR kit master mix (New England Biolabs, Inc., Ipswitch, MA), 4 μl of primer mix and 6 μl of either water (control) or DNA. The primer mix contains the forward and reverse primers each at a concentration of 1.5 μM. Genomic DNA stocks were made from either pure cultures of the parental (GZ3639) and mutant strains (dAC or dMat) or from genomic DNA extracted from wheat seed. Genomic DNA stocks of 100 μl from pure cultures were made by serially diluting DNA in 5-fold increments from 100 ng μl^{-1} to 0.000256 ng μl^{-1} in water. Genomic DNA stocks from wheat infected with the dMat strain were diluted to 29 ng μL^{-1}. Each 29 ng μL^{-1} stock was diluted in serial 2-fold dilutions to 128-fold. Genomic DNA from the 32-fold and 128-fold dilutions was used in PCR reactions.

All PCR reactions were run in a DNA Engine Opticon System (BioRad Laboratories, Inc., Hercules, CA) using the following cycling protocol: initial denature at 95 °C for 3 min; 5 cycles of 95 °C for 30 s, 68 °C for 20 s, 72 °C for 45 s, 63 °C for 15 s followed by a plate read; 5 cycles of 95 °C for 30 s, 66 °C for 20 s, 72 °C for 45 s, 63 °C for 15 s followed by a plate read; 26 cycles of 95 °C for 30 s, 64 °C for 20 s, 72 °C for 45 s, 63 °C for 15 s followed by a plate read. A melting curve analysis followed the cycling protocol in which fluorescent reads were acquired every 0.2 °C starting at 30 °C and ending at 95 °C with a 1 s hold between reads. For standard curve generation, the threshold was set at 0.02769.

2.7. Standard curve production

PCR reactions were performed in triplicate on template DNA concentrations ranging from 120 ng to 0.00154 ng in serial 5-fold dilutions. The cycle number at which the amplification curves cross the threshold set at 0.02769 was determined. From these CT values, average was calculated and plotted as a function of the Log_{10} of the template input amount in nanograms. Outliers were not included in the generation of standard curves.

2.8. Outlier analysis

An experimental CT value data point was determined to be an outlier if it was outside the mean CT value by ±0.5 (Bustin and Nolan, 2004b). This was confirmed by plotting all the data points as CT value vs. Log_{10} of template input amount in nanograms. Putative outliers in these plots clearly deviated from the linear trend. If the CT values from one or two of the three experiments were outside the mean CT value ±0.5, then the curve generated in the absence of that data point was compared to a curve containing the data point. If the curves were superimposable regardless of the inclusion or exclusion of the suspect data point, the data point was not defined as an outlier. If the two curves were not

superimposable, the data point was defined as an outlier and not used in the generation of the standard curve.

3. Results

3.1. Optimization of the fluorescence acquisition temperature

The PCR cycling parameters were modified from those developed for the Fg16 primers (Nicholson et al., 1998) by including a 15 s incubation at 63 °C followed by a fluorescence read (plate read). This fluorescent read temperature was determined from a gradient PCR protocol with an incubation step of 15 s ranging from 61 °C to 85 °C inserted after the extension step (72 °C for 45 s) in each cycle. PCR reactions with or without template DNA plus the Fg16 primers were run and the resulting amplification plots and melt curves were analyzed. The Fg16 primers were chosen for determining the plate read temperature primarily because the melting temperature of the 410 bp Fg16F/R amplicon with a GC content of 47% was predicted to be lower than the 400 bp HygF/R amplicon with a GC content of 59%. Background fluorescence at a plate read temperature of 63 °C was minimal and gave a good amplification curve in the presence of 5 ng of *F. graminearum* DNA.

The end-products resulting from this protocol at various plate read temperatures were also analyzed from melting curves over a temperature range of 30 °C to 95 °C (Fig. 1). Reactions without added template show a non-specific peak spanning 72 °C to 77 °C (Fig. 1(a)). Based on the absence of this peak in reactions with template, it is likely due to primer–dimers rather than contaminating DNA (Fig. 1(b)). Unlike the traces at 61 °C, 62 °C, and 65 °C, the trace at 63 °C does not have the primer–dimer peak (Fig. 1(a)) and in the presence of DNA, the left-hand shoulder is the most narrow (Fig. 1 (b)). These results establish the specificity of the cycling protocol with a fluorescent read temperature at 63 °C.

3.2. Primer specificity

Real-time PCR was carried out under this optimized cycling protocol using the Fg16F/R and the Hyg primers in the absence or presence of 4.8 ng wild-type or transformant DNA to examine the primer specificity. The amplification plots using the Fg16F/R primers showed virtually no background. Three experiments using 4.8 ng of each DNA source revealed CT values with a mean of 18.6 and a standard deviation of 0.375. This similarity of the amplification curves establishes the reliability of our method for determining the DNA concentration in our stock preparations and the consistency of the Fg16 primers with different *F. graminearum* template DNAs. End product melt curve analysis revealed a single sharp peak with an average melting temperature of 83 °C and a standard deviation of 0.245. No peaks were present in the absence of *F. graminearum* DNA. These results confirm the specificity of the Fg16 primers (Nicholson et al., 1998) and establish their specificity under our real-time conditions.

The melting curve using the Hyg primers in the absence of DNA showed a small peak spanning 74 °C to 77 °C. In the presence of transformant DNA (dAC or dMat), containing the hygromycin resistance gene, a strong peak spanning 84 °C to 89 °C was observed (Fig. 2). The absence of the peak at 74 °C to 77 °C in the presence of transformant DNA suggests that this peak is from the formation of primer–dimers. When wild-type DNA was used as a template at concentrations less than or equal to 0.192 ng, a product with a melting temperature that overlaps the primer–dimer peak was evident. The inclusion of more than 0.192 ng of wild-type DNA led to additional peaks including one overlapping the specific transformant DNA peak. The loss of these peaks in the presence of transformant DNA (containing the *HYG* gene) indicates that the Hyg primers do bind nonspecifically to an unknown wild-type DNA sequence but with low affinity. It is important to note that the fluorescence generated by this nonspecific PCR product does not influence the CT value as a comparison of amplification curves with and without this background fluorescence subtracted had essentially identical CT values (data not shown).

Real time PCR with the Hyg and the Fg16 primers on a mixture of equal amounts (2.5 ng) of wild-type and dMat genomic DNA further demonstrated their specificity. The Fg16 primers should amplify sequence from genomic DNA of both strains while the Hyg primers should only amplify sequence from dMat genomic DNA. Therefore, the Fg16 primers should yield 2-fold more products than the Hyg primers reflected by a difference between the CT values of 1. We found that the Fg16 primers generated a CT value of 21.97 and the Hyg primers generated a CT value of 23.05 with a fold difference ($2^{\Delta CT}$ or $2^{1.08}$) of 2.11 which agreed well with the expected value.

3.3. Primer reproducibility

Three experiments were performed with either wild-type or transformant DNA isolated from pure mycelium to examine the reproducibility of the Fg16 primers. PCR reactions were conducted with DNA template amounts

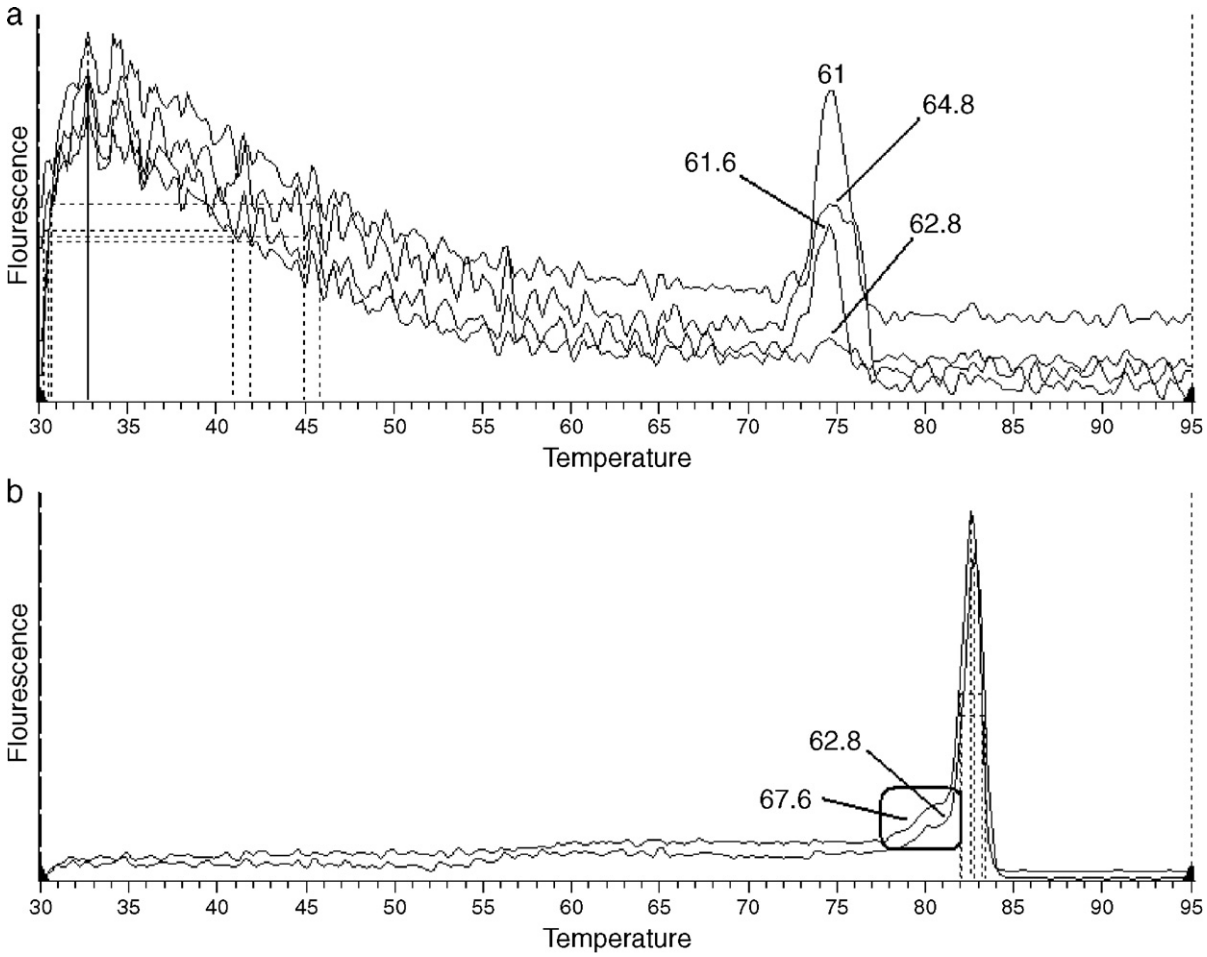

Fig. 1. Optimization of fluorescent read temperature: melting curve analysis. (a) Primer–dimer peaks spanning 72 °C to 77 °C are evident from melting curves for PCR reactions containing the Fg16 primers but lacking template DNA and with plate read temperatures different than the optimal temperature of 62.8 °C. The range of peak heights from the negative first derivative of the fluorescent intensity ($-dI/dT$) was 0.002828 to 0.004574. (b) Specific product peaks spanning 81 °C to 84 °C are seen from melting curves for PCR reactions containing template genomic DNA with the Fg16 primers. An optimal narrow peak, indicated by the window highlighting the left-hand shoulder, is seen with a plate read temperature of 62.8 °C. PCR reaction and cycling conditions are identical to those in (a) except that 5 ng of GZ3639 genomic DNA is included with each reaction. The range of peak heights from the negative first derivative of the fluorescent intensity ($-dI/dT$) was 0.03808 to 0.04358. The numbers in both figures highlight specific traces and indicate the temperature (°C) at which a fluorescent reading (plate read) was taken after incubation for 15 s.

ranging from 120 ng to 0.00154 ng in serial 5-fold dilutions. The resulting amplification curves from each experiment at each dilution were compared and the cycle number at which the curves cross the threshold was noted. If the assay is reproducible, the cycle number at which the curves cross the threshold (CT value) should be similar for each experiment.

Wild-type DNA (GZ3639) was titrated against a constant amount of Fg16F/R primers and subjected to our optimized real-time PCR protocol. Excluding the 120 ng data point ($Log_{10}=2.08$) having a standard deviation of 1.3, the replicate experiments for the dilution series revealed agreeable CT values with standard deviations from the mean equal to or less than 0.934. Despite some scatter at the 0.038 ng data point ($Log_{10}=-1.42$), the mean CT value is tightly associated with the linear standard curve (Fig. 3). The larger standard deviations from the mean CT value for the 0.038 ng and 120 ng amounts of DNA input were due mainly to the second experiment which contributed 60% and 65% of the variation, respectively. This indicates researcher error rather than error inherent in the assay.

When dMat genomic DNA is used as a template for the Fg16 primers, standard deviations from the mean CT value from three experiments were less than or equal to 0.657 except for the 24 ng data point ($Log_{10}=1.38$). This data point showed a deviation of 4.99 due almost

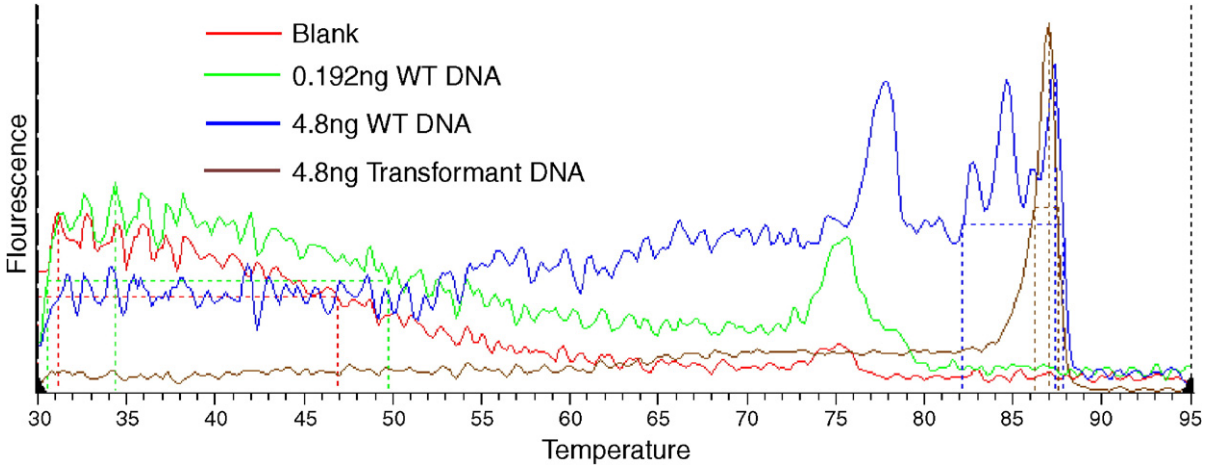

Fig. 2. Specificity of Hyg primers under the optimized cycling protocol. Melting curve analysis on products generated using the Hyg primers with wild-type (WT, GZ3639) genomic DNA gives non-specific peaks spanning 73 °C to 89 °C. The number and intensity of the peaks is directly proportional to the amount of wild-type template in the reaction. The melting curve obtained when transformant genomic DNA (dAC) is used as a template shows one specific peak spanning 84 °C to 89 °C. This indicates that the Hyg gene, present in the transformant, effectively competes for the non-specific binding of the Hyg primers to the wild-type sequence. The range of peak heights from the negative first derivative of the fluorescent intensity ($-dI/dT$) is 0.003501 to 0.02221. Blank indicates that genomic DNA template was not included in the reaction.

exclusively to experiment 1, which contributed 66.4% of the variation. Again, this demonstrates introduced rather than inherent error. Removal of this outlier results in a curve with a high correlation coefficient and with good agreement to the GZ3639 curve (Fig. 3).

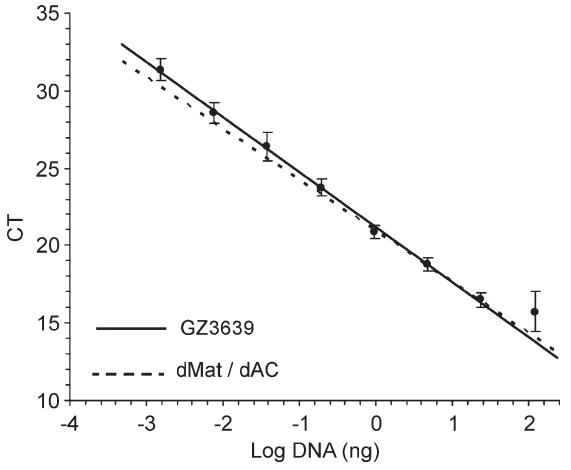

Fig. 3. Reproducibility of the Fg16 primers. PCR reactions were performed with the Fg16 primers and wild-type genomic DNA (GZ3639) or transformant genomic DNA (dAC or dMAT) as template. PCR reactions were performed in triplicate on template genomic DNA concentrations ranging from 120 ng ($Log_{10}=2.08$) to 0.001536 ng ($Log_{10}=-2.81$) in serial 5-fold dilutions. The error bars represent the standard deviation from the mean for the GZ3639 standard curve. For clarity, only the data points for the GZ3639 curve are shown. Excluding outliers, the data points from the dMat and dAC curves had standard deviations less than the 0.0077 ng data point ($Log_{10}=-2.11$) from the GZ3639 curve. The dAC curve is superimposable with the dMat curve. The equations from the three curves are as follows: GZ3639, $y=-3.5584x+21.19$ ($R^2=0.9986$); dMat, $y=-3.3110x+20.9641$ ($R^2=0.9985$); dAC, $y=-3.3135x+21.135$ ($R^2=0.9963$).

The 5-fold dilution series from 120 ng to 0.0384 ng of dAC DNA generated standard deviations from the mean CT value of 0.54 or less. Standard deviations for the 0.00154 ng ($Log_{10}=-2.81$) and 0.0077 ng ($Log_{10}=-2.11$) amounts were larger (1.37 and 1.83, respectively) with one experiment accounting for the majority of the variation. Removal of both of these outliers resulted in a curve with a strong correlation coefficient and almost identical equations (Fig. 3).

Overall, these experiments demonstrate the reproducibility of this protocol with the Fg16F/R primers. Excluding outliers, standard deviations for the CT values generated from nine experiments with the Fg16 primers from all three DNA sources ranged from a low of 1.02% of the mean to a high of 3.54% of the mean. Deviations in CT values were noted for some data points with each DNA source in only one of the three experiments indicating researcher error rather than error inherent in the assay.

Six experiments with transformant DNA as a template with the Hyg primers also generated similar CT values (Fig. 4). The highest standard deviation from the mean CT value for the dMat DNA was 0.888 for the 0.192 ng ($Log_{10}=-0.717$) data point. We did not consider this data point an outlier because its removal does not significantly alter the slope of the standard curve. The highest standard deviation from the mean CT value for dAC DNA was 0.449 from the 7.68 pg data point ($Log_{10}=-2.11$). A plot of the mean CT values for

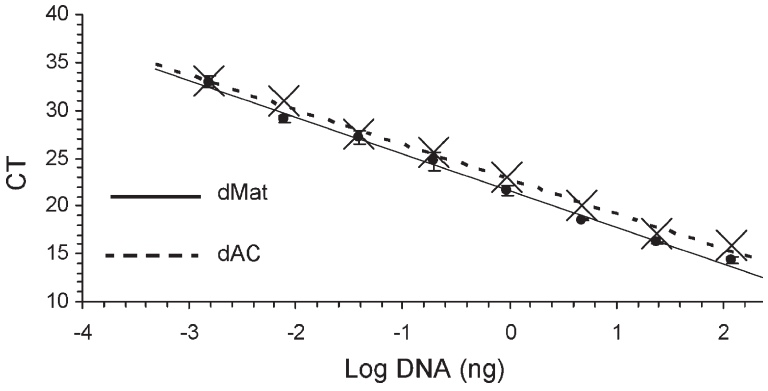

Fig. 4. Reproducibility of the Hyg primers. PCR reactions were performed with the Hyg primers and transformant DNA (dAC or dMAT) as template. PCR reactions were performed in triplicate on template DNA concentrations ranging from 120 ng (Log_{10}=2.08) to 0.001536 ng (Log_{10}=−2.81) in serial 5-fold dilutions. The filled circles represent the data points for the dMat curve while the "×" represents data points for the dAC curve. For clarity, only error bars for the dMat curve are shown. The error bars represent the standard deviation from the mean CT value from three experiments. The data points from the dAC curve had standard deviations less than the 0.96 ng data point (Log_{10}=−0.0177) from the dMat curve. The equations from the two curves are as follows: dMat, $y=-3.8201x+21.668$ (R^2=0.9954); dAC, $y=-3.6304x+22.812$ (R^2=0.9953).

the dilution series from 120 ng to 0.00154 ng of both transformants DNAs show good agreement (Fig. 4). Over all, the standard deviations from the mean for the CT values generated from the six experiments ranged from a low of 0.064% to a high of 3.6%.

3.4. Measurement of quantitative confidence

In order to access the confidence in the quantification of our assay, we generated template DNA from wheat infected with the dMat strain. PCR with 1.36 ng and 5.44 ng of template DNA generated CT values from the Fg16 and Hyg primers that were very close with standard deviations of only 0.279 and 0.016, respectively (Table 1). These close CT values translate to high confidence in the calculated mass of fungal DNA which comprises between 0.034% to 0.044% of the total DNA input (Table 1).

When 1.36 ng of template DNA is assayed using either primer pair, the calculated mass of fungal DNA is beyond the limit of our standard curve but the quantitative confidence is still 77% (Table 1). At 5.44 ng of total DNA input, the calculated amount of fungal DNA from the CT values of both primer pairs is within the lower limit of our standard curve giving a quantitative confidence of 98.6% (Table 1).

Table 1
Quantitative confidence of the protocol

	1.36 ng of total DNA input		5.44 ng of total DNA input	
	Fg16 primers	Hyg primers	Fg16 primers	Hyg primers
CT[a]	33.042 (32.845±0.279)	32.647	30.614 (30.603±0.016)	30.5918
Fungal DNA mass (pg)[b]	0.467 (0.535±0.0962)	0.603	2.247 (2.263±0.0226)	2.279
% Fungal DNA[c]	0.0343	0.0443	0.0413	0.0419
Quantitative confidence[d]	77.4%		98.6%	

[a] The mean CT (threshold cycle) and standard deviation are shown in parentheses.

[b] The mass of fungal DNA was calculated from the formula, $x=1000[10^{\{(y-b)/m\}}]$ where y is the experimental CT value and b and m are the y-intercept (21.19) and slope (−3.5584) in the standard curve equation of $y=-3.5584x+21.19$. The mean and standard deviation are shown in parentheses.

[c] The % fungal DNA is the calculated mass divided by the total input DNA multiplied by 100.

[d] The Quantitative confidence is calculated by dividing the mass of fungal DNA from the Fg16 primers by the mass of fungal DNA from the Hyg primers and multiplying that result by 100.

4. Discussion

Significant progress has been made in understanding the infection process of *F. graminearum* on wheat (Guenther and Trail, 2005; Miller et al., 2004; Ribichich et al., 2000; Skadsen and Hohn, 2004). The impact of rapid advances in fungal genomic technologies is beginning to be felt as numerous new candidate genes potentially involved in disease are being identified (Kruger et al., 2002; Pritsch et al., 2000; Pritsch et al., 2001; Trail et al., 2003). Unfortunately, functional analysis studies are lagging. A full understanding of the role a gene may play in disease has to include gene deletion studies. To date, the *TRI5* or trichodiene synthase gene (Proctor et al., 1995), two map kinases (Hou et al., 2002; Jenczmionka et al., 2003) a non-

ribosomal peptide synthase (Lu et al., 2003), a lipase (Voigt et al., 2005), a cystathionine beta-lyase, a methionine synthase (Seong et al., 2005) and the *TRI14* gene of unknown function (Dyer et al., 2005) have all been disrupted using a hygromycin-based selection system. The *HYG* gene encodes the enzyme hygromycin-B phosphotransferase which confers resistance to the antifungal compound hygromycin (Fincham, 1989). Initial experiments to assess the ability of each mutant to cause disease were carried out with wheat in greenhouse assays. To date, experiments to assess disease in the field have been conducted with only the *TRI5* mutant strain. Field trials are critical to a complete understanding of the role fungal genes play in virulence. Interpretation of previous field studies with the *TRI5* knockout were complicated by the significant background infection by naturally-occurring *F. graminearum* strains containing a wild-type TRI5 gene (Bai et al., 2001).

We have developed a real-time quantitative PCR protocol that allows for the quantitation of both wild-type and hygromycin-based knockout strains in parallel. Although we found our assay to be reproducible, outlier analysis was crucial for identifying faulty data resulting from researcher error. To minimize such error, all aspects of the assay should be standardized including the method and reagents for DNA extraction and purification, the reagents used for PCR and the machine and software used for running the samples and analyzing the results. While setting up the PCR assay, minimal pipetting should be the goal. Stock mixes containing the primers, PCR reagents, and water should be made so that they can be aliquoted together followed by the addition of template. The generation of standard curves with each experiment is necessary to ensure accurate comparison between experiments.

Our method has a number of advantages over other recently developed real-time quantitative PCR protocols that utilize SYBR green (Schnerr et al., 2001; Schnerr et al., 2002) or based on probes (Reischer et al., 2004; Waalwijk et al., 2004). The major advantage of SYBR green-based assays is that they are significantly cheaper than probe-based assays (Bustin and Nolan, 2004a). Although probe-based assays are considered more sensitive than DNA binding dyes like SYBR green, we found our method to be comparable to a recently described probe-based study with *F. graminearum* (Waalwijk et al., 2004).

The major improvement of our protocol compared to another SYBR green-based protocol is a significantly higher sensitivity. Specifically, our protocol is reproducibly quantitative to 1.54 pg of standard DNA which is an order of magnitude more sensitive than the most recent optimized assay by Schnerr et al. (2002). This increase in sensitivity is comparable to recently described probe-based protocols (Waalwijk et al., 2004; Reischer et al., 2004). In these studies, researchers report consistent quantitative results down to 0.9 pg and 0.4 pg, respectively. Compared to our SYBR green assay, this translates to a 1.7-fold and 3.9-fold increase in sensitivity, respectively.

It is important to note that the use of the two primer sets with our protocol allowed us to assess fungal DNA content in as little as 0.5 pg of DNA extracted from plant material with significant confidence (Table 1). In this experiment, 1.36 ng of total input DNA generated CT values of 33.04 with the Fg16 primers and 32.6 with the Hyg primers. The calculated fungal DNA mass values based on the standard curve were very similar (Table 1). The similarity of the DNA values generated by both primer sets increases significantly when total input DNA was increased 4-fold to 5.44 ng. At this level of total DNA input, the confidence in fungal DNA mass calculation increases to 98.6% (Table 1).

In conclusion, we have developed a simple, highly reproducible and accurate real-time quantitative PCR assay that allows for the direct comparison of wild-type and mutant strains during assessment of virulence in the greenhouse or in the field. This will allow investigators to better understand the role that specific genes play in the disease process which, in turn will assist in identifying potential targets of control for Fusarium head blight caused by *F. graminearum*.

Acknowledgments

We thank Elizabeth Mays and Richard Stessman for technical assistance.

References

Bai, G.-H., Shaner, G., 1994. Scab of wheat: prospects for control. Plant Dis. 78, 760–766.

Bai, G.-H., Shaner, G., 1996. Variation in *Fusarium graminearum* and cultivar resistance in wheat scab. Plant Dis. 80, 975–979.

Bai, G.-H., Desjardins, A.E., Plattner, R.D., 2001. Deoxynivalenol-nonproducing *Fusarium graminearum* causes initial infection, but does not cause disease spread in wheat spikes. Mycopathologia 153, 91–98.

Bowden, R.L., Leslie, J.F., 1992. Nitrate non-utilizing mutants of *Gibberella zeae* and their use in determining vegetative compatibility. Exp. Mycol. 16, 308–315.

Bustin, S.A., Nolan, T., 2004a. Chemistries. In: Bustin, S.A. (Ed.), A–Z of Quantitative PCR. International University Line, La Jolla, CA, pp. 215–263.

Bustin, S.A., Nolan, T., 2004b. Data analysis and interpretation. In: Bustin, S.A. (Ed.), A–Z of Quantitative PCR. International University Line, La Jolla, CA, pp. 441–482.

Brown, D.W., Dyer, R.B., McCormick, S.P., Kendra, D.F., Plattner, R. D., 2004. Functional demarcation of the *Fusarium* core trichothecene gene cluster. Fungal Genet. Biol. 41, 454–462.

Desjardins, A.E., Proctor, R.H., Bai, G.-H., McCormick, S.P., Shaner, G., Buechley, G., Hohn, T.M., 1996. Reduced virulence of trichothecene-nonproducing mutants of *Gibberella zeae* in wheat field tests. Mol. Plant-Microb. Interact. 9 (9), 775–781.

Desjardins, A.E., Bai, G.-H., Plattner, R.D., Proctor, R.H., 2000. Analysis of aberrant virulence of *Gibberella zeae* following transformation-mediated complementation of a trichothecene-deficient (*tri5*) mutant. Microbiology 146 (8), 2059–2068.

Desjardins, A.E., Brown, D.W., Yun, S.-H., Proctor, R.H., Lee, T., Plattner, R.D., Lu, S.-W., Turgeon, G.B., 2004. Deletion and complementation of the mating type (*MAT*) locus of the wheat head blight pathogen *Gibberella zeae*. Appl. Environ. Microbiol. 70, 2437–2444.

Dyer, R.B., Plattner, R.D., Kendra, D.F., Brown, D.W., 2005. *Fusarium graminearum* TRI14 is required for high virulence and DON production on wheat but not for DON synthesis *in vitro*. J. Agric. Food Chem. 53, 9281–9287.

Fincham, J.R.S., 1989. Transformation in fungi. Microbiol. Rev. 53, 148–170.

Guenther, J.C., Trail, F., 2005. The development and differentiation of *Gibberella zeae* (anamorph: *Fusarium graminearum*) during colonization of wheat. Mycologia 97 (1), 229–237.

Hou, Z., Xue, C., Peng, Y., Katan, T., Kistler, H.C., Xu, J.-R., 2002. A mitogen-activated protein kinase gene (MGV1) in *Fusarium graminearum* is required for female fertility, heterokaryon formation and plant infection. Mol. Plant-Microb. Interact. 15 (11), 1119–1127.

Jenczmionka, N.J., Schafer, W., 2004. The GpmK1 kinase of *Fusarium graminearum* regulates the induction of specific secreted enzymes. Curr. Genet. 47, 29–36.

Jenczmionka, N.J., Maier, F.J., Losch, A.P., Schafer, W., 2003. Mating, conidiation and pathogenicity of *Fusarium graminearum*, the main causal agent of the head-blight disease of wheat, are regulated by the MAP kinase gpmk1. Curr. Genet. 43, 87–95.

Kruger, W.M., Pritsch, C., Chao, S., Muehlbauer, G.J., 2002. Functional and comparative bioinformatic analysis of expressed genes from wheat spikes infected with *Fusarium graminearum*. Mol. Plant-Microb. Interact. 15 (5), 445–455.

Lu, S.-W., Kroken, S., Lee, B.-N., Robbertse, B., Churchill, A.C.L., Yoder, O.C., 2003. A novel class of gene controlling virulence in plant pathogenic ascomycete fungi. Proc. Natl. Acad. Sci. U. S. A. 100 (10), 5980–5985.

Miller, J.D., Ewen, M.A., 1997. Toxic effects of deoxynivalenol on ribosomes and tissues of the spring wheat cultivars Frontana and Casavant. Nat. Toxins 5 (6), 234–237.

Miller, S.S., Chabot, D.M.P., Ouellet, T., Harris, L.J., Fedak, G., 2004. Use of a *Fusarium graminearum* strain transformed with green fluorescent protein to study infection in wheat (*Triticum aestivum*). Can. J. Plant Pathol. 26, 453–463.

Nicholson, P., Simpson, D.R., Weston, G., Rezanoor, H., Lees, N., Parry, A.K., Joyce, D.W., 1998. Detection and quantification of *Fusarium culmorum* and *Fusarium graminearum* in cereals using PCR assays. Physiol. Mol. Plant Pathol. 53, 17–37.

Pritsch, C., Muehlbauer, G.J., Bushnell, W.R., Somers, D.A., Vance, C.P., 2000. Fungal development and induction of defense response genes during early infection of wheat spikes by *Fusarium graminearum*. Mol. Plant-Microb. Interact. 13 (2), 159–169.

Pritsch, C., Vance, C.P., Bushnell, W.R., Somers, D.A., Hohn, T.M., Muehlbauer, G.J., 2001. Systemic expression of defense response genes in wheat spikes as a response to *Fusarium graminearum* infection. Physiol. Mol. Plant Pathol. 58, 1–12.

Proctor, R.H., Hohn, T.M., McCormick, S.P., 1995. Reduced virulence of *Gibberella zeae* caused by disruption of a trichothecene toxin biosynthetic gene. Mol. Plant-Microb. Interact. 8 (4), 593–601.

Reischer, G.H., Lemmens, M., Farnleitner, A., Adler, A., Mach, R.L., 2004. Quantification of *Fusarium graminearum* in infected wheat by species specific real-time PCR applying a TaqMan Probe. J. Microbiol. Methods 59, 141–146.

Ribichich, K.F., Lopez, S.E., Vegetti, A.C., 2000. Histopathological spikelet changes produced by *Fusarium graminearum* in susceptible and resistant wheat cultivars. Plant Dis. 84 (7), 794–802.

Rocha, O., Ansari, K., Doohan, F.M., 2005. Effects of trichothecene mycotoxins on eukaryotic cells: a review. Food Addit. Contam. 22 (4), 369–378.

Schnerr, H., Niessen, L., Vogel, R.F., 2001. Real time detection of the *tri5* gene in *Fusarium* species by LightCycler–PCR using SYBR Green I for continuous fluorescence monitoring. Int. J. Food Microbiol. 71, 53–61.

Schnerr, H., Vogel, R.F., Niessen, L., 2002. Correlation between DNA of trichothecene-producing *Fusarium* species and deoxynivalenol concentrations in wheat samples. Lett. Appl. Microbiol. 35, 121–125.

Seong, K., Hou, Z., Tracy, M., Kistler, H.C., Xu, J.-R., 2005. Random insertional mutagenesis identifies genes associated with virulence in the wheat scab fungus *Fusarium graminearum*. Phytopathology 95, 744–750.

Skadsen, R.W., Hohn, T.M., 2004. Use of *Fusarium graminearum* transformed with gfp to follow infection patterns in barley and *Arabidopsis*. Physiol. Mol. Plant Pathol. 64, 45–53.

Snijders, C.H.A., 1990. Fusarium head blight and mycotoxin contamination of wheat, a review. Neth. J. Plant Pathol. 96, 187–198.

Trail, F., Xu, J.-R., San Miguel, P., Halgren, R.G., Kistler, H.C., 2003. Analysis of expressed sequence tags from *Gibberella zea* (anamorph *Fusarium graminearum*). Fungal Genet. Biol. 28, 187–197.

Tuite, J., Shaner, G., Everson, R.J., 1990. Wheat scab in soft red winter wheat in Indiana in 1986 and its relation to some quality measurements. Plant Dis. 74, 959–962.

Urban, M., Mott, E., Farley, T., Hammond-Kosack, K., 2003. The *Fusarium graminearum* MAP1 gene is essential for pathogenicity and development of perithecia. Mol. Plant Pathol. 4 (5), 347–359.

Voigt, C.A., Schafer, W., Salomon, S., 2005. A secreted lipase of *Fusarium graminearum* is a virulence factor required for infection of cereals. Plant J. 42, 364–375.

Waalwijk, C., van der Heide, R., De vries, I., Van der Lee, T., Schoen, C., Costrel-de Corainville, G., Hauser-Hahn, I., Kastelein, P., Kohl, J., Lonnet, P., Demarquet, T., Kema, G.H.J., 2004. Quantitative detection of *Fusarium* species in wheat using TaqMan. Eur. J. Plant Pathol. 110, 481–494.